ChemComm

Cellulose Monolith Supported Metal/Organic Framework as Hierarchical Porous Materials for Flow Reaction

Journal:	*ChemComm*
Manuscript ID	CC-COM-10-2019-008232.R1
Article Type:	Communication

ChemComm

COMMUNICATION

Cellulose Monolith Supported Metal/Organic Framework as Hierarchical Porous Materials for Flow Reaction†

Zhaohang Yang, [a] Taka-Aki Asoh,*[a] and Hiroshi Uyama *[a]

Received 00th January 20xx,
Accepted 00th January 20xx

DOI: 10.1039/x0xx00000x

www.rsc.org/

Cellulose monolith immobilized with controlled growth of metal organic frameworks (MOFs) is developed. The synthesized hierarchical porous monolith has great performance as flow reactor.

Metal–organic frameworks (MOFs), represent a new range of highly ordered porous crystalline materials made up of infinite ordered arrays of metal-ion-based nodes (or clusters containing metals), which have been linked by polydentate organic linkers to form extended networks. Due to the nature of their interactions, rational and versatile assemblies between metal centers and organic ligands allow the tuned MOF to have a number of remarkable properties, like ultrahigh large surface areas, tunable pore sizes and shapes, high porosity, and specific adsorption affinities. In-depth research has been conducted to investigate ways of integrating MOF on solids (e.g., polymer materials, metal or metal oxide particles, plastic, silica etc.) for specific applications. [1-10]

Notably, the coated MOF layers allow the manufacture of "smart" surfaces, which can be modified based on the desired functionality.[11] In particular, the structure of micro- or nanocrystalline MOF layers over proper porous polymer supports provides for the formation of a large variety of new composite materials with a wide range of properties.[12-13] However, little research has been carried out on flow-based applications that utilize porous polymer materials coated with MOFs.

Highly hydrophilic cellulose is one of the most abundant natural polymers. In previous study, we have discussed that monoliths made of cellulose can be well supplied with water and chemically modified.[14] Cellulose monoliths (CMs) are seen as outstanding supports for flow-based applications in the sense that they are remarkably stable, easy to prepare, freely molded into varied shapes, less expensive and highly permeable to flow.[15-16] MOFs conjugated cellulose monoliths have not been described before. The Traditional layer-by-layer (LbL) approach, based on liquid phase epitaxy,[17-21] only works when incorporating the MOF onto planar substrates or the surface of particles, revealing remarkable limitations for the case of polymer monoliths possessing a variety of internal skeletons. Moreover, this method is cumbersome and time-consuming.

In this study, we prepared novel cellulose monolith supported MOF as hierarchical porous materials for flow reaction. The assembled MOF layers demonstrated to have both intrinsic microporosity and mesoporosity, and exerting the functional properties of the internal porous network of pristine cellulose monolith. This MOF/cellulose monolith possesses various distinguished properties such as high water holding capacity, improved chemical and mechanical stability and high flow-through ability. ZIF-8, a subclass of MOFs, was selected as a prototype material mainly because of its reproducible straightforward synthesis and intrinsic microporosity.[22-23] The exact value of the synthesized ordered macro-microporous ZIF-8-coated conjugate monolith is examined by flow-through microreactor heterogeneous catalysis.

ZIF-8/cellulose monoliths were prepared as shown in Fig. 1 a. In brief, cellulose monolith with suitable anchoring sites for the growth of ZIF-8 was firstly obtained via free-radical polymerization of sodium *p*-styrene sulfonate in the presence of acryloyl group-introduced cellulose monolith. Then controlled growth of ZIF-8 layers was performed on the pores of monolith by pumping ZIF-8 precursor which is prepared by mixing methanolic $Zn(NO_3)_2{\cdot}6H_2O$ and 2-methylimidazole (HmIm) methanolic solutions. The nucleation effect of different metal and ligand concentration of ZIF-8 precursor on sulfonate-decorated monolith was discussed in this work. Details are described in Table S1. Fig. 1 b-e present the cross-sectional micrographs of polyelectrolyte modified cellulose monolith (C-*g*-PSS) and ZIF-8 conjugated cellulose monolith (ZIF-8@PSS). It showed that there were noticeable morphological differences

[a] *Department of Applied Chemistry, Graduate School of Engineering, Osaka University, Yamadaoka 2-1, Suita, Osaka 565-0871, Japan. E-mail: asoh@chem.eng.osaka-u.ac.jp uyama@chem.eng.osaka-u.ac.jp*

†Electronic Supplementary Information (ESI) available: Experimental details, FTIR data and NMR analytical data. See DOI: 10.1039/x0xx00000x

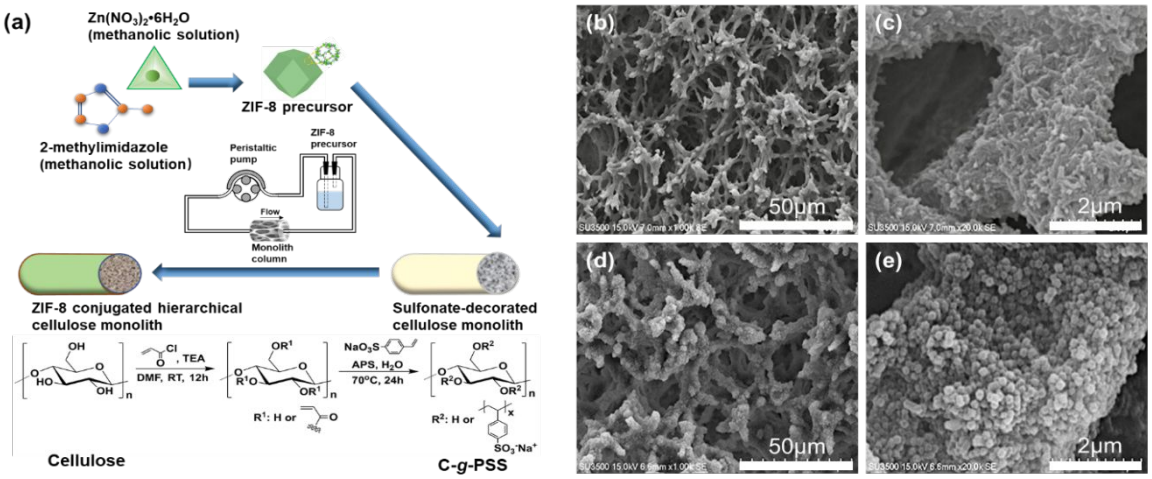

Fig. 1 (a) Schematic diagram of synthesis and fabrication of ZIF-8 conjugated cellulose monolith; (b, c) cross-sectional SEM images of C-*g*-PSS monolith; (d, e) ZIF-8@PSS monolith prepared by pump injection method at flow rate of 1mL min^{-1} for 30 min.

between C-*g*-PSS and ZIF-8@PSS monoliths. C-*g*-PSS monolith had a continuous three-dimensional porous network. This type of morphology is similar to that of the bare cellulose monolith. When pumping the ZIF-8 precursor, the ZIF-8 crystals were uniformly and compactly coated on the surface and internal skeleton of the monolith without causing any damage to the network. The aggregated and well-shaped crystals constituting the ZIF-8 layers had an average size of approximately 200 nm, which made the monolith skeleton to have a bigger diameter. The C-*g*-PSS monolith allowed a large number of anionic sulfonate moieties to be exposed to the contact interface. The great capacity of anionic sulfonate for uptake and exchange of Zn^{2+} cations led to the nucleation, deposition and growth of ZIF-8 on the internal skeleton. Once the ZIF-8 layer had grown, subsequent sequential crystallization growth of MOF multilayers was triggered by flow-based ZIF-8 precursor during a preset growth time. We can observe the growth of ZIF-8 layers on both surface and internal skeleton of the monolith as shown in Fig. S1 f. While cellulose monolith itself doesn't have functional sites to anchor ZIF-8 nanoparticles, as shown in Fig. S2. Compared with LbL methods, this flow-based strategy allows for the homogeneous and heterogeneous nucleation and deposition of ZIF-8 propulsion, which achieves thick highly crystalline layers at high deposition rates. We also found that the mechanical strength showed considerable improvement for the filling of the macropores with ZIF-8 particles (Fig. S3). In addition, we performed the same experiment to anchor the UiO-66 MOF, and similarly obtained the UiO-66 hybrid cellulose monolith. We have confirmed the crystallization growth of UiO-66 in the pores of cellulose monoliths by SEM and XRD analysis (Fig. S1 and Fig. S4).

Further, an XPS experiment was conducted to demonstrate the ability of the C-*g*-PSS monolith to coordinate the Zn^{2+} ions present in the flow-based ZIF-8 precursor solution. High resolution characterization confirmed the presence of Zn^{2+} ions in the ZIF-8@PSS monolith after pumping the ZIF-8 precursor solution into the as-synthesized, Na^{+}-coordinated C-*g*-PSS monolith for 30 min at a flow rate of 1 mL min^{-1} (Fig. S5). It can be observed that the values founded for C 1s, Zn 2p and N 1s are similar to previously reported XPS binding energies peak for ZIF-8.[24] This indicates that, in the presence of Zn^{2+} ion-rich solutions, ion exchange occurs at a certain flow rate. This means that Na^{+} ions are removed from the macromolecular environment of the C-*g*-PSS monolith and subsequently replaced by Zn^{2+} ions.

The change of texture was illustrated by means of nitrogen adsorption-desorption isotherms. The C-*g*-PSS monolith was predominantly mesoporous (2-50 nm) and macroporous (>50 nm), showing properties of a type IV isotherm with a pronounced hysteresis loop of type H3 in terms of IUPAC classification of isotherms (Fig. 2 a). It also exhibited a low surface area and wider pore size distribution. Coating with ZIF-8 layer showed properties of a type I isotherm, and the drastic increase in the volume adsorbed at very low relative pressures is due to the presence of micropores (Fig. 2 b). This was also confirmed by the pore size distribution with an average pore size of 2.4 nm based on the Density Functional Theory (DFT) method, which indicates that the porosity of the composite is mainly attributed to the ZIF-8 component. The growth of ZIF-8 layers also led to a dramatic increase in the BET surface area of ZIF-8-0.2f@PSS (pump injection flow rate of 0.2 mL min^{-1}) and ZIF-8-1f@PSS (flow rate of 1 mL min^{-1}) monoliths up to 228 m^2 g^{-1} and 262 m^2 g^{-1}, respectively, as shown in Table S2. The increment of the surface area is due to the deposition and growth of ZIF-8 on the surface of the monolith skeleton, which results in an increase of the total pore volume. Obviously, during the same pump injection time, the specific surface area

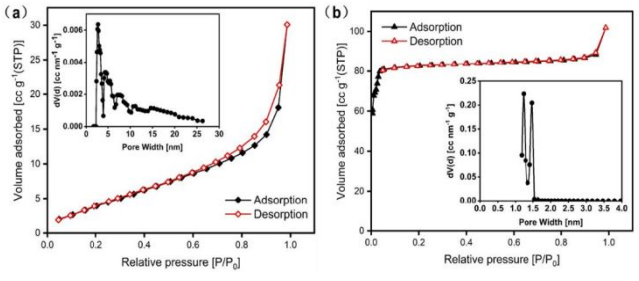

Fig. 2 Nitrogen adsorption/desorption isotherms of (a) C-*g*-PSS monolith and (b) ZIF-8@PSS monolith (preparation time: 30 min; flow rate: 1 mL min^{-1}). Inset: pore size distribution plots.

of the monoliths can be adjusted by the flow rate and positively correlated with it.

We further performed experiments to assess the influence of pump injection time and flow rate on the binding amount of the ZIF-8 nanoparticles on the signal formation in single particle inductively coupled plasma mass spectrometry (spICP-MS) measurements by using dispersions containing zinc nanoparticles. Here, the dried ZIF-8@PSS monolith (15 mg), completely dissolved in aqua regia, was prepared for testing. The results showed that the content of zinc in the monolith is positively correlated with both the pump injection time and flow rate. This implies that at the same flow rate, the longer the injection time, the higher the amounts of ZIF-8 nanoparticles in the coating. Then, at the same injection time, the zinc content increases with an increase of the flow rate. In other words, the preparation time can be decreased by increasing the injection flow rate (Table S3). It is the sufficiently exposed sulfonate groups that give the zinc ions a strong adsorption capacity for the monolith at low concentration of ZIF-8 precursor (3.5 mM, 10 mL). The adsorption content reached 9.7 wt% at a flow rate of 1.5 mL min^{-1} and a pump injection time of 30 minutes. Combining with the discussion above, it is feasible that the coated amount of MOF and the surface area of the monoliths can be regulated by both the pump injection time and flow rate on a need basis.

The average measurements of pressure loss at a water flow rate of 1, 2 and 3 mL min^{-1} were successively used to calculate the permeability coefficient B_0. In order to reduce the deviation caused by backpressure, we analyzed the pressure loss by utilizing the average of the three measurements. As can be seen in Fig. 3, with a ZIF-8 coating, the permeability of the monolith will be reduced, and the reduction will be more pronounced in case the flow rate or pump injection time are increased. The explanation for this phenomenon is simple; increasing the flow rate or pump injection time subsequently increases the amount of monolith interface in contact with ZIF-8. ZIF-8 was allowed to grow on the surface of internal skeleton of the monolith layer by layer. It is the gradually thickened ZIF-8 layers that narrowed the monolith pores, thereby reducing the permeability. We have noticed that there was a linear increase in the pressure drop as the flow rate or pump injection time increased. Optimization of the flow rate and pump injection time is vital in practical application as it ensures the monolith structure will not collapse in the event of significant pressure drop. Meanwhile, coating with adequate and homogeneous MOF layers is also important.

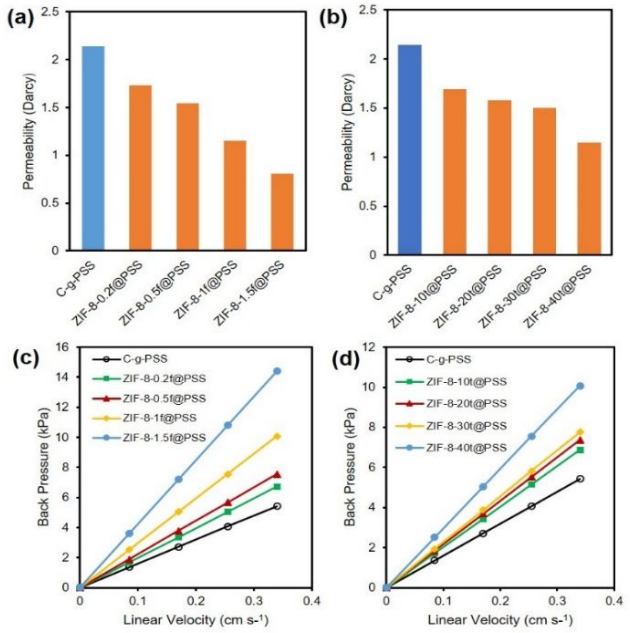

Fig. 3 (a, b) Average permeability measurements of C-*g*-PSS and ZIF-8@PSS monoliths at flow rate of 1, 2 and 3mL min^{-1}; (c, d) Calculated back pressure at different linear velocity. (D: 5 mm, L:10 mm).

ZIF-8 has been noted to be an effective catalyst for Knoevenagel condensation reaction, which is an important synthesis route for fine chemicals and many pharmaceuticals. Research has established that catalyst loading is positively correlated to quantitative conversion rate.[25] Meanwhile, it is possible to regulate the ZIF-8 particles loaded in our monolith by increasing the pump injection time and flow rate. In this stage, we prepared a C-*g*-PSS monolith in a 100 mm-long tubing with an inner diameter of 5 mm, and coated it with ZIF-8 using the pump injection method at a flow rate of 1.5 mL min^{-1} for 30 min. This was done to exemplify its use as a micro flow-through reactor for catalyzing the Knoevenagel reaction of benzaldehyde with ethyl cyanoacetate (Fig 4 a). More details about the same are provided in the Supporting Information. Firstly, a batch reaction was conducted to assess whether there are any comparisons between ZIF-8 crystals and the ZIF-8@PSS monolith for the purpose of revealing the role ZIF-8 plays in the catalytic reaction. As shown in Table 1, for the same amount of ZIF-8, the ZIF-8@PSS monolith exhibits similar catalytic activity as the ZIF-8 crystals. Knoevenagel condensation reaction with ZIF-8-free PSS monolith provided the conversion of 8.4 % benzaldehyde and a desired product yield of 3.0 % at the reaction time of 30 min. ZIF-8 is regarded as an efficient base catalyst which originates from the 2-methylimidazole ligand. We also established that the presence of the ZIF-8@PSS monolith in the flow microreactor speeded up the reaction rate and almost attained complete conversion after only 5 min, which is more than 3 times as high as with the batch condition (Fig. 4 b). This reaction was also authenticated by H^1NMR. As highlighted in Fig. S6, ZIF-8@PSS monolith microreactor achieved the highest conversion of benzaldehyde up to 99 %, and yield of the desired product up to 93 % after reaction time of 20 min. Compared with batch reaction (TOF= 609 h^{-1}), this microreactor exhibited extremely high catalytic efficiency (TOF=4616 h^{-1}, almost 7 times higher than batch reaction) and long-term stability. The enhanced catalytic performance of the ZIF-8@PSS monolith can thus be credited to the augmentation of the reaction rate by the microreactor and the greater efficiency of the nanosized ZIF-8 crystals coated on the

Table 1 Benzaldehyde conversion of 20 mg ZIF-8@PSS monolith (about 1.9 mg ZIF-8), 1.9 mg bulk ZIF-8 and 20 mg C-*g*-PSS monolith for 9 mL reactant mixture in the batch reaction.

Catalyst	Reaction time (min)					
	5	10	15	20	25	30
ZIF-8@PSS	48.7%	75.3%	81.6%	83.9%	84.5%	85.9%
Bulk ZIF-8	49.3%	74.0%	80.8%	83.5%	84.8%	85.0%
C-*g*-PSS	0.3%	5.0%	6.5%	7.2%	7.8%	8.4%

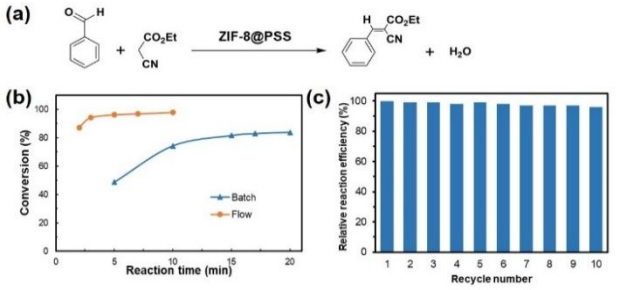

Fig. 4 (a) Knoevenagel reaction of benzaldehyde with ethyl cyanoacetate (Reaction conditions: 20 mg of ZIF-8@PSS monolith, calculated $n_{catalyst}$=0.03 mmol, 32 mmol of benzaldehyde and 32 mmol of ethyl cyanoacetate in DMSO at 60 °C; (b) Conversion of the Knoevenagel condensation reaction in flow mode and batch catalysis mode using ZIF-8@PSS monolith microreactor; (c) The reusability of ZIF-8@PSS monolith for Knoevenagel reaction.

monolith. The leaching of catalytic particles is the most censorious flaw of continuous-flow microreactors because it will eventually lead to momentous catalyst loss and contamination of the product stream. Fig. 4 c shows details of the analysis of the stability and reusability of the ZIF-8@PSS monolith microreactor. It can be seen that there was 99% catalytic conversion for the first 5 times, and only decreased by 4% past the 10th time. The actual amounts of ZIF-8 before and after 10 recycling times were analyzed through ICP-MS. The results showed that negligible reduction of Zn was obtained (before: 9.70 wt.%, after: 9.69 wt.%). The slow decrease in catalytic performance might be due to some micro pores/channel in monolith are closed due to the continued back pressure in the flow process. In addition, negligible reduction of Zn was detected, indicating that almost no catalyst loss during the experiment. It is anticipated that the majority of the catalytic activity takes place on the surface of the ZIF-8 crystals. The C-*g*-PSS monolith itself has a certain catalytic ability compared with blank (＜2%), the integration of ZIF-8 and C-*g*-PSS monolith thereby intensifies the catalytic activity in flow reaction. This form of nanoparticle encapsulation in C-*g*-PSS monolith can also be applied in other catalytic processes.

In conclusion, we have anchored MOF within the pores of monolithic cellulose with exposed pre-defined chemical moieties using a modest and articulate approach. The proposed strategy is acquiescent to fast preparation of nanoparticle/polymer monolith conjugates under mild conditions. By taking advantage of the affinity of Zn^{2+} ions for multiple sulfonate moieties, we examined how the ZIF-8 coating can be enhanced through a pump injection method. These plastic composite materials have been reported to be effective for flow-through microreactor catalysis. As a catalysis microreactor, ZIF-8 can provide for quicker and higher conversion while maintaining outstanding stability and reusability. Based on the affinity of metal ions of MOFs for anionic sulfonate moieties, we believe the proposed approach can prove beneficial for the propulsion growth of other MOFs on anionic polyelectrolyte modified polymer monolith in a rather controllable manner.

This work was supported by JSPS KAKENHI Grant Numbers 17H03114, 19H02778, JST-Mirai Program Grant Number JPMJMI18E3, Japan and JSPS Core-to-Core Program, B. Asia-Africa Science Platforms.

Conflicts of interest

There are no conflicts to declare.

Notes and references

1 Y. Lv, X. Tan, F. Svec, *J. Sep. Sci.* 2017, **40**, 272-287.
2 Q. Fu, L. Wen, L. Zhang, X. Chen, D. Pun, A. Ahmed, Y. Yang, and H. Zhang. *ACS. Appl. Mater. Interfaces.* 2017, **9**, 33979-33988.
3 S. Lirio, W. Liu, C. Lin, H , Huang. J. *Chromatogr. A.* 2016, **1428**, 236-245.
4 A. Saeed, F. Maya, D. J. Xiao, M. Najam, F. Svec, D.K.Britt. Adv. Fun*ct. Mater*. 2014, **24**, 5790-5797.
5 J. Zhuang, D. Ar, X. Yu, J. Liu, A. Terfort. Ad*v. Mater*. 2013, **25**, 4631-4635.
6 Z. Li, H. C. Zeng, *Am. Chem. Soc.* 2014. **136**, 5631-5639.
7 J. Kou and L.-B. Sun, *ACS. Appl. Mater. Interfaces*. 2018, **10**,12051-12059.
8 T. Zhang, X. Zhang, X. Yan, L. Kong, G. Zhang, H. Liu, J. Qiu, K. L. Yeung. *Chem. Eng. J.* 2013, **228**, 398-404.
9 G. M. Segovia, J. S. Tuninetti, S. Moya, A. S. Picco, M. R. Ceolín, O. Azzaroni, M. Rafti. *Mater. Today Chem.* 2018, **8**, 29-35.
10 M. Matsumoto, T. Kitaoka，*Adv. Mater*. 2015, **28**, 1765-1769.
11 A. Betard, R. A. Fischer, *Chem Rev.* 2011, **112**, 1055-1083.
12 L. Wen, A. Gao, Y. Cao, F. Svec, T. Tan, Y. Lv. *Macromol. Rapid Commun.* 2016, **37**, 551-557.
13 M. Ghani, S. Masoum, S. M. Ghoreishi, V. Cerdà, and F. Maya. *J. Chromatogr. A.* 2018, **1567**, 55-63.
14 Z. Yang, T.-A. Asoh, and H. Uyama. *Bul.l Chem. Soc. Jpn*, 2019, **92**, 1453-1461.
15 T. Jin, C. D. Easton, H. Yin, M. de Vries, and X. Hao, *Sci Technol Adv Mater*, 2018, **19**, 381-395.
16 M. A. Lucchini, E. Lizundia, S. Moser, M. Niederberger, and G. Nyström, *ACS. Appl. Mater. Interfaces*. 2018, **10**, 29599-29607.
17 S. Yang, F. Ye, C. Zhang, S. Shen, S. Zhao. *Analyst.* 2015, **140**, 2755-2761.
18 O. Shekhah, L. Fu, R. Sougrat, Y. Belmabkhout, A. J. Cairns, E. P. Giannelis, and M. Eddaoudi. *Chem. Commun*. 2012, **48**, 11434.
19 D. Jiang, A. D. Burrows, R. Jaber, and K. J. Edler. *Chem. Commun*. 2012, **48**, 4965.
20 Y. Li, X. Zhang, X. Chen, K. Tang, Q. Meng, C. Shen, and G. Zhang, *ACS. Appl. Mater. Interfaces*. 2019, **11**, 12605-12612.
21 C. Zhang, Y. Li, H. Wang, S. He, Y. Xu, C. Zhong, and T. Li, *Chem Sci*, 2018, **9**, 5672-5678.
22 G. Lu, S. Li, Z. Guo, O. K. Farha, B. G. Hauser, X. Qi and J.S. DuChene. *Nat. Chem*. 2012, **4**, 310.
23 Y. Pan, Y. Liu, G. Zeng, L. Zhao and Z. Lai. *Chem. Commun*. 2011, **47**, 2071.
24 M. Rafti, J. A. Allegretto, G. M. Segovia, J. S. Tuninetti, J. M. Giussi, E. Bindini, and O. Azzaroni. *Mater. Chem. Front.* 2017, **1**,2256-2260.
25 U. P. N. Tran, K. K. A. Le, N. T. S. Phan, *ACS. Catalysis*. 2011, **1**, 120-127.

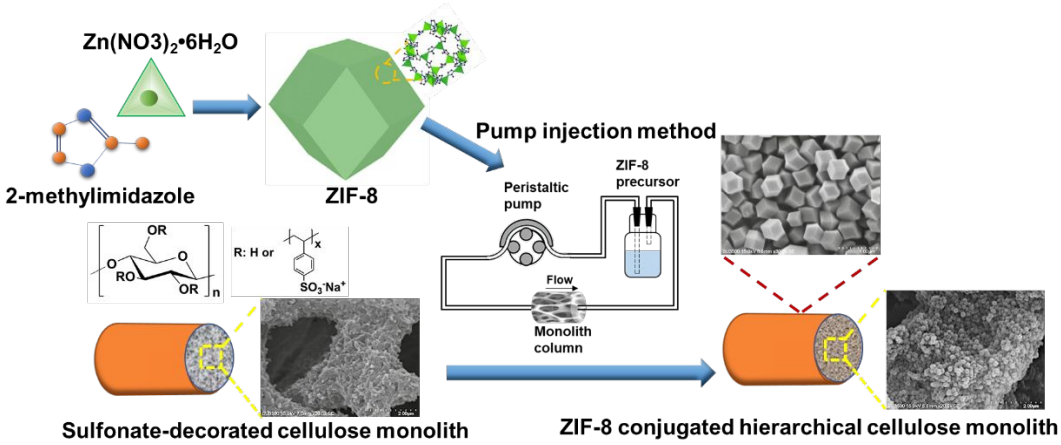

A novel cellulose monolith supported ZIF-8 metal organic framework as hierarchical porous material was designed by using a highly effective pump injection method, which is used for the flow-based reaction.